Impact of chemical treatments on the molecular and stable carbon isotopic composition of sporomorphs

Yannick F. Bats[1], Klaas G.J. Nierop[1], Alice Stuart-Lee[1], Joost Frieling[1§], Linda van Roij[1], Gert-Jan Reichart[1,2], Appy Sluijs[1]

[1]Department of Earth Sciences, Faculty of Geosciences, Utrecht University, Princetonlaan 8, 3584 CB Utrecht, The Netherlands
[2]NIOZ Royal Netherlands Institute for Sea Research, 1797 SZ 't Horntje, the Netherlands
§ now at: Department of Earth Sciences, University of Oxford, South Parks Road, OX1 3AN, Oxford, United Kingdom

Correspondence to: Yannick F. Bats (y.f.bats@uu.nl)

Abstract. The stable carbon isotope composition ($\delta^{13}C$) of plants and algae is influenced by environmental factors, such as $p\text{CO}_2$, water availability, and altitude. To effectively use the $\delta^{13}C$ of fossil material as proxies for these parameters, it is essential to understand the chemical and isotopic effects of diagenesis and conventional chemical treatments. In this study, we subject various species of pollen and spores of higher plants to different chemical treatments simulating diagenesis and chemical alteration in the environment as well as palynological processing. We analyze changes in molecular and isotopic composition, using pyrolysis gas chromatography – mass spectrometry (MS), and both elemental analyzer and laser ablation isotope ratio MS, respectively. We find that saponification removes extractable and ester-bound lipids, which increases the $\delta^{13}C$ value of the sporomorphs. Treatment with HF and HCl removed most hydrolysable polysaccharides and proteins, causing a drop in $\delta^{13}C$ values. Acetolysis produced aromatic-rich residual sporomorphs with the lowest $\delta^{13}C$ values compared to other treatments, likely representing the diagenetically resistant sporopollenin polymer. These findings imply a successional depletion of ^{13}C during fossil maturation, where aliphatic lipids are diagenetically removed in the process, until only the relatively ^{13}C depleted sporopollenin remains. To adequately compare fossil and extant sporomorph $\delta^{13}C$ values, we advise the use of HF-HCl and a lipid removal step other than acetolysis as palynological treatment, as acetolysis treats the material non-uniformly. Lastly, laser ablation-IRMS shows promise for targeted isotopic analysis of individual specimens of various types of palynomorphs.

1 Introduction

The stable carbon isotopic composition ($\delta^{13}C$) of (sub-)fossil organic microfossils – such as pollen, dinoflagellate cysts, larval eggshells, acritarchs, and chironomid head capsules – are increasingly used as proxies in environmental and ecological reconstructions, for example to infer C_4 versus C_3 grass abundance, atmospheric $p\text{CO}_2$, and diet (e.g., Kaufman & Xiao, 2003; Nelson et al., 2007; Schilder et al., 2018; Sluijs et al., 2018; van Hardenbroek et al., 2018). The mechanistic and statistical underpinning of $\delta^{13}C$-based proxies is often based on controlled growth experiments or field studies linking the isotopic

composition of the source organism to a specific variable (e.g., Loader and Hemming, 2004; van Hardenbroek et al., 2010; Hoins et al., 2015). However, when during taphonomy these organisms transform into their fossilizable remains, they undergo

35 *post-mortem* chemical alteration, also referred to as diagenetic alteration, which potentially affects their $\delta^{13}C$ composition (e.g., Benner et al., 1987; Loader and Hemming, 2004). In addition, these fossil remains typically undergo some type of palynological treatment before analysis, which often includes strong acids and might further affect their macromolecular composition and hence $\delta^{13}C$ values (e.g., Amundson et al., 1997; Müller et al., 2021). As a consequence, the molecular composition of a processed fossil is typically biased towards the most resistant organic compounds. Therefore, laboratory

40 experiments as well as modern calibration field studies must include similar chemical treatment to link the $\delta^{13}C$ values measured on extant and fossil sporomorphs.

Organic microfossils are comprised of organic macromolecular structures such as sporopollenin (the main component of exine – the outer wall of pollen and spores), residual labile compounds (e.g., polysaccharides, proteins) and diagenetically produced 'geopolymers' that become enriched over time and are only susceptible to strong oxidation (De Leeuw et al., 2006;

45 Quilichini et al., 2015). However, in addition to the exine, extant sporomorphs often also contain pectin and (hemi)cellulose as well as attached lipids, proteins and sugars (Fan et al., 2019). Such components all have their own inherent stable isotopic signature which may differ strongly in $\delta^{13}C$ from the mean exine value. Although this implies that their relative contribution potentially strongly impacts the overall stable isotopic composition, these more labile components are typically consumed or oxidized in the environment before sporomorphs are buried in sediments so that only the exine is preserved. Furthermore, it

50 has been suggested that lipids may bind to the microfossils *post-mortem* in the sedimentary record (Van Bergen et al., 1993; De Leeuw et al., 2006; Versteegh et al., 2007), influencing the integrated stable carbon isotopic signal.

Palynological treatment is commonly required to concentrate organic microfossils from sediments. Treatments typically include HCl to dissolve inorganic carbon phases and HF to dissolve siliceous materials. Acetolysis (acetic acid used together with acetic anhydride and H_2SO_4), KOH and NaClO are sometimes used, notably in terrestrial settings, to remove (amorphous)

55 organic matter components and stain pollen walls. Several studies have shown that acetolysis strongly changes sporomorph $\delta^{13}C$ (Amundson et al., 1997; Descolas-Gros and Schölzel, 2007; Müller et al., 2021). Also other steps, including HF-HCl and oxidants, may remove labile organic components and therefore potentially affect the $\delta^{13}C$ of the remaining palynomorphs (Müller et al., 2021). Such steps therefore also essentially simulate the effects of natural ageing and environmental oxidation.

After early $\delta^{13}C$ analyses of spores (Murphey and Nier, 1941), it took decades before pollen were targeted for $\delta^{13}C$ analyses,

60 notably with the aim to distinguish C_3 from C_4 carbon acquisition pathways using total combustion isotope ratio mass spectrometry (IRMS) (Amundson et al., 1997). Such early work needed large numbers of specimens for precise and accurate analyses. More recent work has optimized cryotrapping and subsequent release of CO_2 following combustion in an Elemental Analyzer (EA) so that much less material is needed for analyses (Polissar et al., 2009). Other devices utilize a continuous (He) flow approach, thereby further minimizing blank contamination before CO_2 is introduced into the IRMS. These include the

65 use of a moving wire to introduce pollen – stuck to the wire – into an oxidation furnace, after which CO_2 is carried on an He flow to an IRMS (Sessions et al., 2005; Nelson et al., 2007). More recently, a continuous flow technique was developed that

carries molecular fragments derived from microfossil laser-ablation (LA) on a He flow into a capillary to a micro combustion oven in which they are oxidized, followed by gas chromatography (GC) and IRMS (Van Roij et al., 2017). The latter technique allows for single specimen $\delta^{13}C$ analyses – similar to the ion microprobe technique used by Kaufman and Xiao, (2003) – and has been applied to pollen (Van Roij et al., 2017), lacustrine *Daphnia* resting eggshells (Schilder et al., 2018) and marine dinoflagellate cysts (Frieling et al., 2023; Sluijs et al., 2018).

Here, we aim to contribute to the existing literature regarding chemically induced $\delta^{13}C$ change of raw sporomorphs by carrying out a series of experiments on raw pollen derived from multiple species. We apply acetolysis, HF-HCl, and saponification to study the individual effects of these common palynological treatment steps and also evaluate this in relation to similar transformation that might occur during taphonomy (diagenesis). We assess the character of chemical alteration resulting from the treatments using pyrolysis gas chromatography – mass spectrometry (GC-MS). Finally, we analyze sporomorphs using conventional EA-IRMS as well as LA – nano combustion (nC) – GC – IRMS to assess analytical consistency.

2 Materials and Methods

2.1 Samples

Six sporomorph species were selected for this study. Concentrated pollen samples of a C_3 grass (*Lolium perenne*), a C_4 grass (*Zea mays*), a gymnosperm tree (*Pinus echinata*), and two angiosperm trees (*Betula pendula*, *Eucalyptus globulus*) were obtained from Greer Labs (Lenoir, USA). A spore sample (*Lycopodium clavatum*) was obtained from Baldwins (London, UK). For the rest of this article the species are referred to by their genus name.

2.2 Treatments

Three different treatments were carried out on each sporomorph species in triplicate. These treatments included HF-HCl, a common acid treatment in palynology to concentrate sporomorphs from mineral samples, saponification to remove ester-bound fatty acids (cf. Nierop et al., 2019), and acetolysis to remove polysaccharides and proteins to yield sporopollenin only (Erdtman, 1960; Hesse and Waha, 1989).

Saponification

In accordance with Nierop et al. (2019), sporomorphs were saponified in 1M KOH in MeOH at 70 °C for 2 h in an oven. After cooling to room temperature, the solution was acidified to pH 3 using 2N HCl. Then dichloromethane (DCM) was added and the whole mixture was thoroughly shaken using a Wilten Vortex Genie apparatus. After phase separation, both the aqueous and the organic layers were removed, and both water and DCM were added to purify the remaining sporomorphs. After thoroughly shaking by the vortex apparatus followed by phase separation, both layers were removed again and this procedure

was repeated twice. MeOH was added to the sporomorphs to remove traces of both water and DCM. This was done twice after which the remaining sporomorphs were dried using a very gentle stream of N_2.

     HF-HCl

Samples of 200 mg untreated pollen were treated with 15 mL 38–40% HF. The samples were placed on a platform shaker for 120 minutes and centrifuged for 5 minutes at 2200 rpm. The supernatant was removed with a glass pipette and the pellet disintegrated on a vortexer. 15 mL of 30% HCl was added to each, followed by a further centrifuge step and separation of the liquid fraction. Distilled water rinses and centrifugation steps were repeated until the samples tested pH neutral, after which

 they were dried in an oven at 60°C for 72 hours and subsequently stored at room temperature until analyses.

      Acetolysis

Samples of 200 mg untreated pollen were treated with 5 mL 99.6% acetic acid, which were then centrifuged for 5 minutes at 2000 rpm. 5 mL of a mixture of pure acetic anhydride and 95-97% sulfuric acid (9:1 volume/volume) was added and the

 samples were placed in a hot water bath at 100°C for 5 minutes, and from there transferred to a cold water bath for 5 minutes. Following centrifugation, the solution was decanted, and the vials vortexed. Four rinsing steps were carried out, adding 12 mL of water, centrifuging, decanting and vortexing. Samples were then dried in an oven at 60°C for 72 hours and stored at room temperature until analyses.

2.3 Pyrolysis-gas chromatography-mass spectrometry (Py-GC-MS)

 Analytical pyrolyses were carried out on a Horizon Instruments Curie-Point pyrolyser. Samples (typically 0.5 mg) were pressed onto Ni/Fe Curie point wires and subsequently heated for 5 s at 600 °C. The pyrolysis unit was directly connected to a Carlo Erba GC8060 gas chromatograph and the products were separated by a fused silica column (Varian, 30 m, 0.32 mm inner diameter) coated with CP-Sil5 (film thickness 0.40 µm). Helium was used as carrier gas. The GC column was directly connected to the pyrolysis unit through a splitless injector set at 280°C. The oven was initially kept at 40°C for 1 min, next it

 was heated at a rate of 7°C/min to 320°C and maintained at that temperature for 15 min. The column was coupled to a Fisons MD800 mass spectrometer (mass range m/z 45–650, ionization energy 70 eV, cycle time 0.7 s). Identification of compounds was carried out based on their mass spectra using a NIST library or by interpretation of the spectra, by their retention times and/or by comparison with literature data.

      All samples were run at least in duplicate. Semi-quantification of the compounds identified was performed by

 integration of peaks using one or two target fragment ions. Correction for this to match total ion chromatogram (TIC) peaks was achieved using the relative response of the fragment ions relative to TIC peaks by integration of well resolved TIC peaks in chromatograms of the samples. The standard (milled oak roots) run was used to check the performance of the Py-GC-MS. The relative abundance of each pyrolysis product was calculated from the sum of all integrated and corrected peak areas. All

correction factors and relative abundances can be found in the Supplementary Data. These data reflect averages of all replicates per pollen and treatment types.

2.4 Stable carbon isotopic analyses

2.4.1 EA-IRMS

Of each untreated and treated replicate, 50 µg was weighed in tin capsules for bulk $\delta^{13}C$ analysis on an elemental analyzer (Thermoscientific Flash 2000) coupled to an IRMS (ThermoFinnigan Delta V Advantage IRMS; short: EA-IRMS) at NIOZ Royal Netherlands Institute for Sea Research. Series of analyses were bracketed by blanks (empty capsules), and Vienna Pee Dee Belemnite (VPDB) calibrated internal standards (nicotinamide, $\delta^{13}C$ -33.48‰; and a sediment standard graphite quartzite (GQ), $\delta^{13}C$ -26.68‰) for calibration to the VPDB scale and to correct for drift. The standard deviation of the GQ standard (0.07‰) represents the analytical error of the EA-IRMS method and is incorporated into the total uncertainty of the sporomorph $\delta^{13}C$ measurements. Considering other authors (e.g., Hemsley et al., 1993) have suggested acetolysis to treat material non-homogeneously, the acetolyzed *Pinus*, *Lolium*, and *Zea* replicates were measured in triplicate (i.e., a triplicate of the triplicates), to assess the treatment's uniformity.

2.4.2 LA-nC-GC-IRMS

One sample for each species and treatment combination (i.e., one of the triplicates) was blindly chosen and analyzed using the approach first described in Van Roij et al. (2017): laser ablation, nano combustion gas chromatography and isotope ratio mass spectrometry (LA – nC – GC – IRMS; for the rest of this article abbreviated to LA-IRMS). Sporomorph grains from each sample were pressed onto a nickel disc using a hydraulic press. A polyethylene (PE) standard (IAEA-CH-7, $\delta^{13}C$ -32.15‰) was added, and the disc placed into an ablation chamber specifically designed for the purpose (Van Roij et al., 2017). Individual grains were targeted using a deep ultraviolet (DUV) ArF laser (COMPex 102; Lambda Physik, Göttingen, Germany, and, COMPexPro 102; Elemental Scientific Lasers LLC, Bozeman, USA, see Supplement Table S6 for which laser was used per sample) to fragment the organic matter, with the ablated particles then being combusted in a micro furnace and the released CO2 transported to a GC and IRMS (ThermoFinnigan Delta V Advantage IRMS). At least five PE standard measurements were done with each LA-IRMS run, to calibrate $\delta^{13}C$ values using standard bracketing. Van Roij et al. (2017) suggested mismatches between EA- and LA-IRMS measurements to possibly result from single standard bracketing, which prevents correcting for linear mass bias over the full range of $\delta^{13}C$ data. Therefore, to test the linear mass bias of the LA-IRMS method, some samples (Supplement Fig. S8) were additionally corrected with a new VPDB calibrated internal polylactic acid (PLA) standard (Premium Eco Clear Bags, ClearBags, North Las Vegas, USA; -12.63‰). Furthermore, Van Roij et al. (2017) showed measurements to be reliable (i.e., small offset from the value determined by EA-IRMS analyses and smaller standard deviation) with peak areas > ~2 Vs. Therefore some measurements were done by ablating multiple grains.

160   The standard deviations of the LA-IRMS measurements represent both inter-specimen variation within the samples – which is averaged out with the bulk EA-IRMS method – and the analytical error of the LA-IRMS method. The internal analytical error is predicted using the standard deviation of PE measurements with a similar peak area as the respective sporomorph sample (Van Roij et al., 2017) and will be compared with the spread in values observed for the samples.

2.5 Data analysis

165   All data analyses were conducted in R (R Core Team, 2023) using the *dplyr* (François et al., 2023), *tidyr* (Wickham and Girlich, 2024), *ggplot2* (Wickham, 2016), *ggridges* (Wilke, 2024) and *boot* (Canty and Ripley, 2022) packages. For the EA-IRMS $\delta^{13}C$ measurements, the total uncertainty for each species/treatment combination was determined by combining the standard deviation (σ) of the replicate measurements with the analytical error (0.07‰) using quadrature addition ($\sigma_{tot} = \sqrt{[\sigma_{analytical}^2 + \sigma_{replicates}^2]}$). Treated and untreated EA-IRMS samples were compared using student's *t*-test.

170   LA-IRMS $\delta^{13}C$ measurements of each species/treatment combination were weighted according to their peak area (Vs), for two reasons. Firstly, the peak area relates directly to the amount of ablated material in a single measurement (Van Roij et al., 2017), which implies a weighted mean more accurately represents the true sample mean, and, secondly, measurements become more precise as peak areas increase (Van Roij et al., 2017; Frieling et al., 2023), which implies that measurements with a higher peak area are statistically more meaningful. The weighted $\delta^{13}C$ measurement of each species/treatment

175   combination were bootstrapped (*n* = 1000), to elude effects of non-normality in further statistical testing. Bootstrapped means and standard errors of the mean (SEM) were used to compare measurements statistically between the treated and untreated LA-IRMS samples and between LA- and EA-IRMS using Welch's *t*-test. For each species/treatment combination, note that the EA-IRMS data is based on triplicates that underwent the treatment separately, whereas the LA-IRMS data comes from a single, randomly chosen triplicate. Therefore, Welch's *t*-test assesses the probability that a randomly drawn LA-IRMS sample

180   matches the EA-IRMS based population mean, which encompasses the range of $\delta^{13}C$ values across the three separate treatments. Lastly, standard deviations between LA-IRMS sporomorph and PE measurements were compared using an F-test.

3 Results

3.1 Sporomorph pyrolysis products upon treatment

Untreated

185   The pyrolysis products of the sporomorphs studied consist of an array of molecules broadly divided into lipids, aromatic compounds and polysaccharides/proteins-derived components; the latter two are here grouped because of their similar hydrolysable nature. The pyrolysis products of the sporomorphs consist predominantly (65% – 81%) of lipids, between 5% and 36% of aromatics, and between 1% and 23% of polysaccharides and proteins (Fig. 1 and 2, and Supplement Fig. S1).

For lipids, fatty acids such as C_{16} and unsaturated C_{18} fatty acids dominate all untreated sporomorphs (Fig. 2). Other lipids such as odd numbered *n*-alkenes and *n*-alkanes in the range of C_{25}-C_{31} are observed in the pollen of *Betula*, *Zea*, and particularly in those of *Lolium* (Supplement Fig. S2). *Pinus* pollen contain some even numbered *n*-alcohols (C_{24}-C_{28}) (Supplement Fig. S2 and Table S2).

Polysaccharide-derived products predominantly represent levoglucosan (Supplement Fig. S3 and Table S3). Anhydropentose and levomannosan represent pyrolysis markers of the monosaccharides xylose and mannose (Supplement Fig. S3). The relative abundance of polysaccharide-derived pyrolysis products is smallest for intact *Lycopodium* spores (~1%) and largest for *Zea* pollen (~22%), with similar intermediate values for the other pollen types. Nitrogen-bearing pyrolysis products include benzyl nitrile, methylbenzyl nitrile, indole and 3-methylindole, and are detected in all species (Supplement Fig. S3), although in small amounts (maximally ~2% for *Eucalyptus*).

For aromatics, typical sporopollenin-derived pyrolysis components are the propionic acid and vinyl (i.e., ethenyl) containing compounds phloretic acid, hydrocaffeic acid, hydroferulic acid, 4-vinylcatechol, 4-vinylphenol and 4-vinylguaiacol (Supplement Fig. S4 and Table S4). The latter two are identified for all species, whereas 4-vinylcatechol only for *Lycopodium*. Phloretic acid is detected in *Pinus* pollen in small amounts, while being absent from all other sporomorph species. Hydrocaffeic and hydroferulic acid are detected in relatively large amounts in *Lycopodium* spores, while absent from other species. Furthermore, the carbonylbenzenes benzaldehyde and acetophenone are consistently observed for all species (Supplement Fig. S4). Other aromatic components present in all species are the methoxyphenols guaiacol (2-methoxyphenol), 4-methyl- and 4-ethylguaiacol (Supplement Fig. S4). The alkylbenzenes styrene, toluene and benzene are also detected for all species (Supplement Fig. S4). Alkylphenols detected in all species consisted of phenol, 2-methylphenol, 3/4-methylphenol and 4-ethylphenol (Supplement Fig. S4).

Saponification

Saponified sporomorphs lose most of their free and ester-bound lipids. Moreover, a large relative increase of polysaccharide-derived components is seen upon saponification, to values of 11% for *Lycopodium* spores, up to 87% for *Lolium* and 89% for *Zea* pollen (Fig. 2 and Supplement Fig. S1). Also the N-bearing components increase relatively (e.g., to ~8% for *Eucalyptus*). A relative increase of aromatic compounds is also witnessed upon saponification, but to a smaller degree than is the case for polysaccharides, suggesting some aromatic compounds are removed by saponification.

HF-HCl

Most, if not all polysaccharides are removed from the sporomorphs by HF-HCl treatment. Also the N-bearing components are not detected anymore (Supplement Fig. S3 and Fig. 1 for *Lolium*). Lipids and aromatics remain similarly abundant in the chemical make-up of the sporomorphs (Fig. 2).

Acetolysis

Acetolysis removes most, if not all *n*-alkanes, *n*-alkenes and alcohols, and reduces the amount of fatty acids substantially. Most polysaccharides are removed upon acetolysis, and N-bearing compounds are also not detected anymore. Only *Zea* retains

225 relatively high amounts of polysaccharides after acetolysis (Fig. 2). A large relative increase of aromatics is observed upon acetolysis. Especially the relative amount of alkylbenzenes and phenol compounds increases with respect to their untreated counterparts (Supplement Fig. S4).

Figure 1. Pyrolysis-gas chromatograms of *Lolium* pollen that were: a) untreated, b) saponified, c) HF-HCl-treated and d) acetolyzed. Colors reflect the retention time intervals with predominantly aromatic (blue), polysaccharide-derived (green)
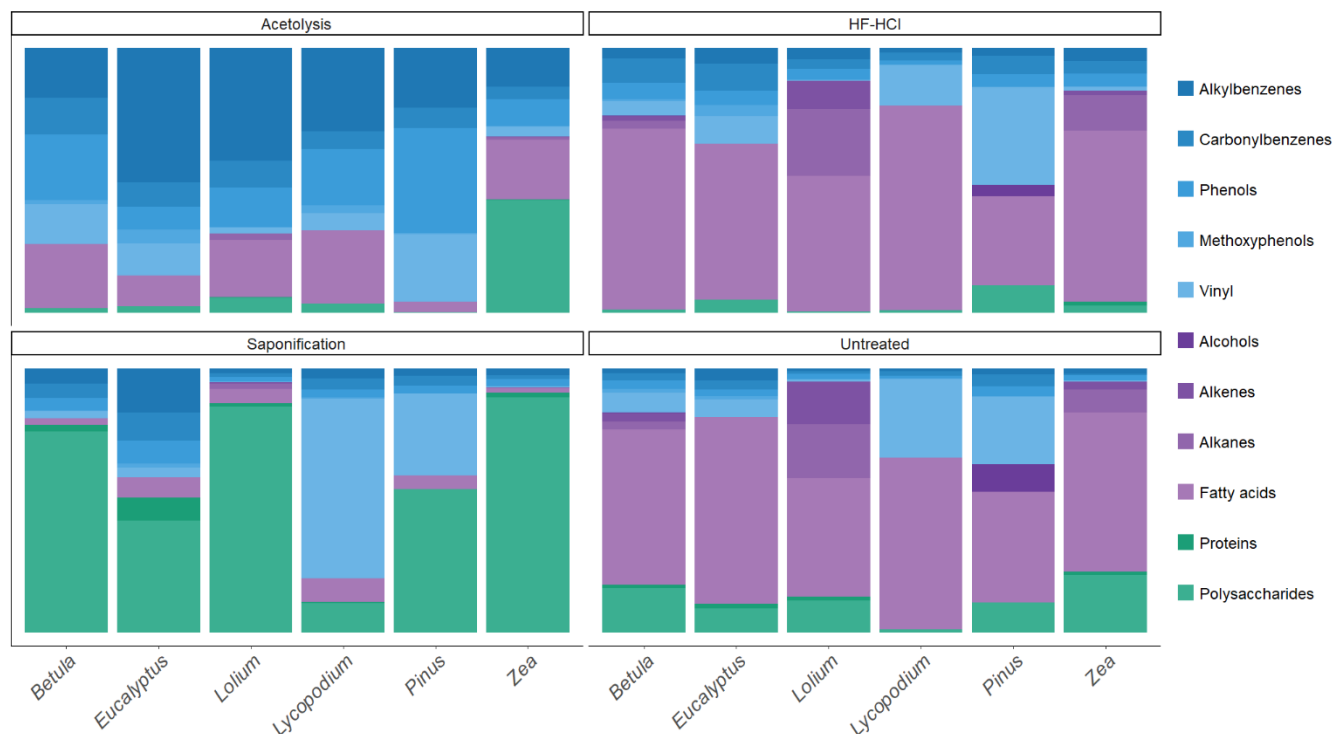
Figure 2. The composition of the various aromatic (blue tints), polysaccharide- and protein-derived (green tints), and lipid
235 (purple tints) pyrolysis products for each species-treatment combination.

3.2 Sporomorph carbon isotope values

3.2.1 EA-IRMS

Untreated

The sporomorph mean δ^{13}C values of the six studied species are presented in Table 1. All untreated sporomorph species have
240 significantly (t-test, all $p < 0.05$) different mean δ^{13}C values compared to each other, except for *Lolium* and *Eucalyptus* ($t = -$
1.52, df = 4, $p > 0.05$) (Supplement Table S5, Fig. 3).

Saponification

Saponification significantly increases δ^{13}C values relative to untreated samples for *Betula*, *Lolium*, *Eucalyptus* and *Zea* (t-test,
245 all $p < 0.05$; Table 1). In contrast, the δ^{13}C values for *Pinus*, and *Lycopodium* do not significantly differ between saponified
and untreated pollen (t-test, all $p > 0.05$; Table 1) (Fig. 3).

HF-HCl

The HF-HCl treatment significantly (t-test, $p < 0.05$) decreases δ^{13}C values across all pollen types compared to untreated
250   sporomorphs (Table 1, Fig. 3). It should be noted that for *Lycopodium* and *Pinus* only a single replicate was measured.

Acetolysis

Acetolysis significantly decreases δ^{13}C values for all sporomorphs compared to the untreated sporomorphs, except for *Zea*
(Table 1, Fig. 3). The triplicates show a substantial range in δ^{13}C values (Fig. 3), especially for *Zea* (-13.5 to 22.0‰), which
255   is the reason there is no statistically significant difference between the acetolyzed and untreated *Zea* sporomorphs.

260

265

270

Table 1. The EA-IRMS stable carbon isotope (δ^{13}C) measurements of each species-treatment combination, and the respective δ^{13}C difference with untreated samples of the same species. A student's *t*-test was performed to compare these differences. Only a single replicate underwent treatment for HF-HCl treated *Lycopodium* and *Pinus*, and therefore no *t*-test was performed for these samples. * = p<0.05, ** = p<0.01, *** = p<0.001.

		EA-IRMS results		Difference versus untreated, *t*-test		
Species	**Treatment**	δ^{13}C	**SD**	**Difference (‰)**	***t*-value**	***p* value**
Zea	Untreated	-12.09	0.22			
Lycopodium	Untreated	-29.78	0.08			
Pinus	Untreated	-28.9	0.10			
Betula	Untreated	-26.02	0.07			
Lolium	Untreated	-28.04	0.13			
Eucalyptus	Untreated	-27.85	0.09			
Zea	HF-HCl	-14.91	0.31	-2.82	-7.44	0.002**
Betula	HF-HCl	-28.97	0.19	-2.95	-14.28	0.0001***
Lolium	HF-HCl	-30.81	0.34	-2.77	-7.65	0.002**
Eucalyptus	HF-HCl	-29.56	0.08	-1.71	-13.93	0.0002***
Lycopodium	HF-HCl	-29.73	NA	NA	NA	NA
Pinus	HF-HCl	-30.07	NA	NA	NA	NA
Zea	Saponification	-10.81	0.08	1.28	5.47	0.005**
Lycopodium	Saponification	-29.75	0.07	0.03	0.24	0.82
Pinus	Saponification	-28.91	0.08	-0.01	-0.08	0.94
Betula	Saponification	-25.77	0.09	0.25	2.25	0.09
Lolium	Saponification	-27.33	0.11	0.71	4.19	0.01**
Eucalyptus	Saponification	-27.48	0.08	0.37	3.06	0.04*
Zea	Acetolysis	-18.03	3.9	-5.94	-1.52	0.2
Lycopodium	Acetolysis	-31.95	0.23	-2.17	-8.89	0.0009***
Pinus	Acetolysis	-32.50	0.24	-3.60	-13.86	0.0002***
Betula	Acetolysis	-31.18	0.30	-5.16	-16.81	0.00007***
Lolium	Acetolysis	-31.14	0.28	-3.10	-10.04	0.0006***
Eucalyptus	Acetolysis	-31.90	0.26	-4.05	-14.68	0.0001***

3.2.2 LA-IRMS

Table 2 shows the results of the LA-IRMS δ^{13}C measurements as compared to the EA-IRMS measurements. Table 3 shows the F-test results of the LA-IRMS standard deviations compared to the analytical error. LA-IRMS samples that are additionally corrected with PLA do not show significantly different results as compared to EA-IRMS, in respect to when they are solely

corrected using PE (Supplement Fig. S8), although there is a linear mass bias involved with the LA-IRMS method (Supplement Fig. S9).
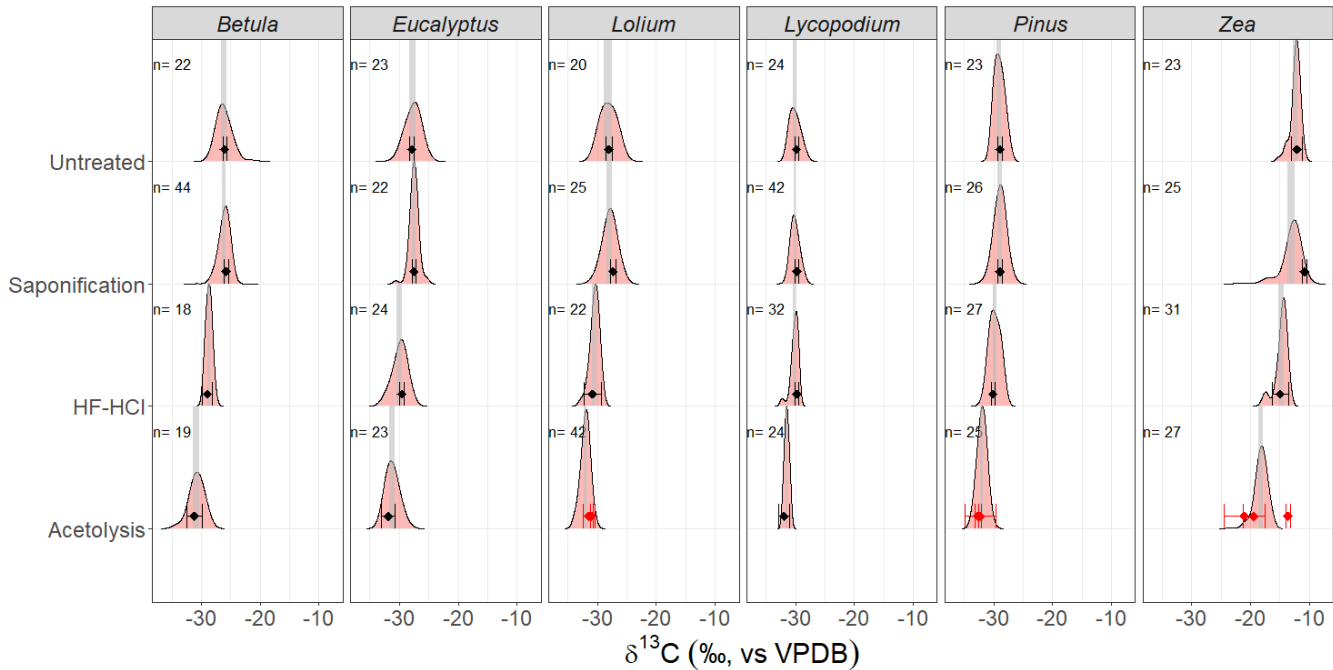
Figure 3. Mean stable carbon isotope ($\delta^{13}C$) and 95% confidence interval (CI) of the EA-IRMS measurements (black points and error bars), and $\delta^{13}C$ distributions of the LA-IRMS measurements (density plots), for each species-treatment combination. Grey shaded areas represent the 95% CI of the mean of the LA-IRMS measurements. Numbers above density plots represent the sample size (i.e., number of LA measurements) of each LA-IRMS sample. The red points and error bars represent the mean stable carbon isotope ($\delta^{13}C$) and 95% CI of triplicates of replicates, showing the non-homogeneous treatment of acetolysis. Note that for HF-HCl treated *Lycopodium* and *Pinus* only a single EA-IRMS measurement has been done (a single replicate), and therefore their respective 95% CIs are based on the 0.07‰ analytical error (see Methods).

Untreated

For each species, the LA-IRMS based $\delta^{13}C$ means of untreated specimens are not significantly different from the $\delta^{13}C$ means obtained using EA-IRMS (*t*-test, all $p > 0.05$; Table 2). Only for *Zea* and *Lolium* standard deviations are significantly larger than the analytical error (F-test, $p < 0.05$; Table 3).

Saponification

300   For *Zea,* the $\delta^{13}C$ means obtained from saponified specimens using LA-IRMS are significantly (*t*-test, $p < 0.05$; Table 2) lower than those obtained using EA-IRMS, with a mean difference of 2.27‰ (Fig. 3). The mean LA-IRMS $\delta^{13}C$ values do not significantly differ between saponified and untreated sporomorphs (*t*-test, all $p > 0.05$; Table 2), even though the EA-IRMS method did reveal a difference for *Zea, Lolium* and *Eucalyptus* (Sect. 3.2.1.). Standard deviations are significantly larger than the analytical error for *Betula, Eucalyptus, Zea* and *Lolium* (F-test, $p < 0.05$; Table 3).

305

       HF-HCl

For each species, the LA-IRMS based $\delta^{13}C$ means of HF-HCl treated specimens are not significantly different from the $\delta^{13}C$ means obtained using EA-IRMS (*t*-test, all $p > 0.05$; Table 2). Standard deviations are significantly larger than the analytical error for *Eucalyptus, Zea* and *Pinus* (F-test, $p < 0.05$; Table 3).

310

       Acetolysis

For each species, the LA-IRMS based $\delta^{13}C$ means of acetolyzed specimens are not significantly different from the $\delta^{13}C$ means obtained using EA-IRMS (*t*-test, all $p > 0.05$; Table 2). All acetolyzed samples have a significantly lower $\delta^{13}C$ than the untreated samples for LA-IRMS (Table 2). Standard deviations are significantly larger than the analytical error for *Betula,*

315   *Eucalyptus, Zea* and *Lolium* (F-test, $p < 0.05$; Table 3).

320

325

Table 2. The LA-IRMS stable carbon isotope (δ^{13}C) measurements of each species-treatment combination, the respective δ^{13}C difference with untreated samples of the same species, and the difference with each sample's corresponding EA-IRMS measurement. Welch's t-tests were performed to compare these differences. * = p<0.05, ** = p<0.01, *** = p<0.001.

LA-IRMS measurements						Welch's t-test (between treated and untreated)				Welch's t-test (between LA- and EA-IRMS)			
Species	Treatment	Mean δ^{13}C (‰)	SD (‰)	n	SEM (‰)	Difference (‰)	t value	df (t-test)	p value	Difference (‰)	t value	df	p value (t-test)
Betula	Acetolysis	-30.8	1.1	19	0.33	-4.7	-10.9	42.68	6.1E-14***	-0.40	-0.91	2.74	4.4E-01
Eucalyptus	Acetolysis	-31.2	1.0	23	0.24	-3.5	-8.6	30.59	1.3E-09***	-0.71	-2.00	2.51	1.6E-01
Lolium	Acetolysis	-32.0	0.75	42	0.13	-3.9	-11.67	7.13	6.7E-06***	0.90	2.92	2.13	9.2E-02
Lycopodium	Acetolysis	-31.5	0.4	24	0.08	-1.4	-7.2	17.06	1.3E-06***	-0.46	-1.89	2.18	1.9E-01
Pinus	Acetolysis	-32.0	0.69	25	0.17	-2.9	-12.2	46.76	4.5E-16***	-0.52	-1.73	2.36	2.1E-01
Zea	Acetolysis	-18.2	1.06	27	0.23	-5.9	-20.3	60.92	7.6E-29***	0.2	0.05	2.03	9.6E-01
Betula	HF-HCl	-28.7	0.51	18	0.13	-2.3	-7.7	15.91	1.0E-06***	-0.27	-1.18	2.43	3.4E-01
Eucalyptus	HF-HCl	-29.9	1.2	24	0.26	-2.3	-5.38	32.80	6.2E-06***	0.38	1.42	3.84	2.3E-01
Lolium	HF-HCl	-30.5	0.78	22	0.19	-2.3	-6.437	21.00	2.2E-06***	-0.31	-0.79	2.3	5.0E-01
Lycopodium	HF-HCl	-30.2	0.67	32	0.12	0.0	0.01	28.34	9.9E-01	0.362	2.58	2.7	9.1E-02
Pinus	HF-HCl	-29.8	0.90	27	0.18	-0.7	-2.64	50.80	1.1E-02*	-0.38	-1.95	3.3	1.4E-01
Zea	HF-HCl	-14.7	1.03	31	0.22	-1.4	-4.75	63.92	1.2E-05***	-0.17	-0.44	2.29	7.0E-01
Betula	Saponification	-26.1	0.84	44	0.14	0.0	0.07	11.83	9.4E-01	0.34	2.05	2.47	1.5E-01
Eucalyptus	Saponification	-27.5	0.79	22	0.19	0.3	0.89	21.15	3.8E-01	0.02	0.12	3.46	9.1E-01
Lolium	Saponification	-27.9	1.17	25	0.28	0.4	0.86	36.03	4.0E-01	0.55	1.88	3.40	1.5E-01
Lycopodium	Saponification	-30.1	0.7	42	0.12	0.0	-0.02	24.35	9.9E-01	0.34	2.43	2.49	1.1E-01
Pinus	Saponification	-28.9	0.92	26	0.20	0.1	0.38	55.99	7.0E-01	0.03	0.14	3.30	8.9E-01
Zea	Saponification	-13.1	1.8	25	0.49	0.1	0.16	89.15	8.8E-01	2.27	4.82	5.73	3.3E-03**
Betula	Untreated	-26.1	1.2	22	0.28					0.11	0.37	4.50	7.3E-01
Eucalyptus	Untreated	-27.7	1.2	23	0.33					-0.16	-0.47	4.24	6.6E-01
Lolium	Untreated	-28.2	1.27	20	0.31					0.12	0.35	3.62	7.5E-01
Lycopodium	Untreated	-30.1	0.84	24	0.17					0.31	1.63	3.21	2.0E-01
Pinus	Untreated	-29.0	0.80	23	0.17					0.14	0.71	2.98	5.3E-01
Zea	Untreated	-12.4	0.8	23	0.18					0.27	0.96	2.44	4.2E-01

330

335

Table 3. LA-IRMS mean peak area and standard deviation (SD) for each species-treatment combination, along with the SD of the PE standard corresponding to the respective mean peak area (Van Roij et al., 2017). An F-test was performed to compare the sample SD with the PE standard SD. * = p<0.05, ** = p<0.01, *** = p<0.001.

Species	Treatment	Mean peak area (Vs)	SD LA	SD PE	F-statistic	df_1	df_2	*p* value
Betula	Acetolysis	1.01	1.14	0.68	2.80	18	40	6.6E-03**
Eucalyptus	Acetolysis	2.47	0.96	0.63	2.33	22	24	4.7E-02*
Lycopodium	Acetolysis	3.32	0.36	0.44	0.68	23	9	4.4E-01
Zea	Acetolysis	6.86	1.06	0.46	5.32	26	27	4.7E-05***
Pinus	Acetolysis	1.31	0.69	0.71	0.95	24	34	9.0E-01
Lolium	Acetolysis	2.88	0.74	0.35	4.45	41	16	2.2E-03**
Betula	HF-HCl	1.19	0.47	0.68	0.48	17	40	1.1E-01
Eucalyptus	HF-HCl	1.02	1.17	0.68	2.99	23	40	2.4E-03**
Lycopodium	HF-HCl	3.91	0.65	0.44	2.17	31	9	2.2E-01
Zea	HF-HCl	6.29	0.80	0.46	3.05	30	27	4.5E-03**
Pinus	HF-HCl	1.75	0.91	0.55	2.71	26	19	2.9E-02*
Lolium	HF-HCl	1.06	0.78	0.68	1.30	21	40	4.6E-01
Betula	Saponification	2.62	0.84	0.35	5.72	43	16	4.5E-04***
Eucalyptus	Saponification	5.76	0.76	0.46	2.73	21	23	2.1E-02*
Lycopodium	Saponification	2.04	0.65	0.63	1.05	41	24	9.1E-01
Zea	Saponification	7.53	1.71	0.39	19.17	25	20	6.7E-09***
Pinus	Saponification	1.41	0.92	0.71	1.68	25	34	1.6E-01
Lolium	Saponification	2.47	1.13	0.63	3.24	24	24	5.6E-03**
Betula	Untreated	0.73	1.15	1.05	1.21	21	20	6.8E-01
Eucalyptus	Untreated	0.76	1.17	1.05	1.24	22	20	6.3E-01
Lycopodium	Untreated	0.97	0.84	0.68	1.51	23	23	3.3E-01
Zea	Untreated	6.54	0.82	0.46	3.18	22	27	5.0E-03**
Pinus	Untreated	1.94	0.80	0.52	2.37	22	21	5.3E-02
Lolium	Untreated	1.32	1.27	0.71	3.18	19	34	3.2E-03**

340 **4 Discussion**

4.1 The overall chemical composition of (un)treated sporomorphs

Untreated

All the untreated sporomorphs are richest in lipids when examined by flash pyrolysis, mostly consisting of C_{16} and C_{18} fatty acids. Polysaccharide- and protein-derived products are the second most abundant compound group in the pollen of *Betula*,

345 *Lolium* and *Zea*, while they are relatively small in *Eucalyptus* and *Pinus*, with only traces found in *Lycopodium* spores. Almost in opposite order are the relative abundances of aromatic pyrolysis products: richest in *Lycopodium* and *Pinus*, followed by *Betula* and *Eucalyptus* and very small abundances in the pollen of *Lolium* and *Zea* (Fig. 2).

Aromatics consist of various alkyl- and methoxyphenols, alkyl- and carbonylbenzenes, and vinyl containing compounds (see section 4.2.). Polysaccharides are dominated by levoglucosan (Fig. S3), a well-known pyrolysis product of cellulose

350 (Pouwels et al., 1987), which forms the main component of the intine of sporomorphs (Shim et al., 2022). Moreover, the presence of xylose- and mannose-derived pyrolysis products suggests the sporomorphs potentially contain a large variety of polysaccharides in addition to cellulose, considering this suite of monosaccharide building blocks. The N-bearing pyrolysis products are all well-known pyrolysis products of proteins (Tsuge and Matsubara, 1985).

It is important to note that the Py-GC-MS method used in this study has a bias toward detecting apolar structures (i.e., 355 the lipids) due to the apolar GC column used. Consequently, polar sugars are under-detected. Whether aromatics are under-represented depends on the degree of polar groups (e.g., COOH, CO, OH) associated with the molecule. However, considering pyrolysis is a well-established method for assessing the chemical composition of organic material, we consider this a robust representation of sporomorph composition, especially when comparing to other studies using pyrolysis.

In sum, untreated sporomorphs are dominated by lipids (i.e., fatty acids) followed by polysaccharides and a mixture of 360 aromatics, with the exact composition varying among the studied species.

Saponification

Upon saponification relative abundances of the extractable and esterified lipids decrease substantially compared to other pyrolysis products (Fig. 2). This treatment not only eliminates alkenes, alkanes, alcohols and fatty acids but also removes some 365 aromatic acids, to varying extents, across all pollen types (Supplement Fig. S4). However, in *Lycopodium*, the aromatic acids (i.e., hydrocaffeic and hydroferulic acid) appear to be relatively persistent (Supplement Fig. S4). The mixture of aliphatic and aromatic compounds removed likely constitutes a significant component of pollenkitt, the sticky substance on pollen and spores that plays a crucial role in *e.g.* the formation of pollen clumps and adherence to pollinators (Pacini & Hesse, 2005).

370 *HF-HCl*

When the sporomorphs are treated with HF-HCl the relative contribution of polysaccharides and proteins becomes small to very small for all HF-HCl treated sporomorphs (Fig. 2), supposedly due to acid-catalyzed hydrolysis of the glycosidic and peptide bonds, respectively. This implies that the HF-HCl treatment effectively removes polysaccharides and proteins. The relative amounts of the lipids detected are hardly affected, likely due to the very polar solvent which prevents solubilization of 375 the lipids, which prefer to stay in the vicinity of the hydrophobic sporomorphs rather than in the aqueous solution.

Acetolysis

Due to the acidic conditions of acetolysis, polysaccharides and proteins are removed, resembling the HF-HCl treatment. Moreover, extractable and hydrolyzed lipids are removed with methanol in the water removal step, leaving sporomorphs rich 380 in aromatic compounds (Fig. 2). These aromatic components detected after acetolysis therefore likely predominantly reflect the pyrolysis products of sporopollenin.

4.2 The aromatic make-up of sporopollenin

Given that the aromatic components present after acetolysis primarily reflect the pyrolysis products of sporopollenin, a more detailed examination of the aromatic composition of sporopollenin is insightful. Nierop et al. (2019) showed that *Lycopodium* spores are rich in cinnamic acid derivatives, such as *p*-coumaric acid, caffeic acid and ferulic acid, and their respective saturated analogues, phloretic acid, hydrocaffeic acid and hydroferulic acid. These components reflect typical sporopollenin-derived components (Jardine et al., 2017, 2021; Li et al., 2019; Lutzke et al., 2020).

Hydroferulic and hydrocaffeic acid are relatively polar structures, which do not have optimal interactions with the apolar GC column used. However, apparently *Lycopodium* produces these compounds in such abundances (Nierop et al., 2019) that they were still detected (Fig. S4).

Upon pyrolysis the unsaturated acids (i.e., *p*-coumaric acid, caffeic acid and ferulic acid) decarboxylate, or when ester-bound yield, 4-vinylphenol, 4-vinylcatechol and 4-vinylguaiacol, respectively, in contrast to the saturated acids (Moldoveanu, 1998). The presence of 4-vinylphenol and 4-vinylguaiacol in all sporomorphs studied here thus suggests their precursors *p*-coumaric acid and ferulic acid to be a consistent component of the sporopollenin polymer for all species. The relative contribution of 4-vinylphenol and 4-vinylguaiacol varied across sporomorph species/treatment combinations in such a way that their precursors *p*-coumaric and ferulic acid must occur in hydrolysable and non-hydrolysable forms.

Based on Thermally assisted Hydrolysis and Methylation-GC-MS (TMH-GC-MS) analyses of spores from eight species of moss, clubmoss, horsetail and fern, as well as pollen from a single cycad species, Nierop et al. (2019) assumed that caffeic acid synthesis in sporomorphs might have been lost during Cycadophyta evolution but was retained in Magnoliophyta (angiosperms). However, 4-vinylcatechol, and thus its precursor caffeic acid, was found only in the clubmoss *Lycopodium*, and was absent from the four angiosperms (*Betula, Lolium, Zea* and *Eucalyptus*), as well as from the gymnosperm *Pinus* (this study) and *Zamia floridana* (Nierop et al., 2019). These findings suggest that caffeic acid synthesis in sporopollenin is specific to spore-producing seedless embryophytes (mosses, clubmosses, liverworts, hornworts, horsetails and ferns) as opposed to pollen-producing seed plants. However, considering the limited amount of taxa studied here, more research is needed to confirm this.

Two other components, benzaldehyde and acetophenone, have been regularly identified in all kinds of samples upon pyrolysis in relatively small abundances (Moldoveanu, 1998). In our spores and pollen these components are found in remarkably high abundances independent of treatment, and are most enriched in the pyrolysates after acetolysis, except for *Eucalyptus* (Fig. S3). Also in the extant megaspores of the lycophyte *Isoëtes killipii* (Boom et al., 2005) and megaspores and massulae of the waterfern *Azolla caroliniana* (Nierop et al, 2011) and in particular in the fossil spores of *Azolla* and *Salvinia* (Van Bergen et al., 1993) both pyrolysis products are prominently present. Furthermore, Boom et al. (2005) synthesized a sporopollenin-like dehydrogenation polymer based on *p*-coumaric acid. Upon pyrolysis this dehydrogenation polymer yielded almost the same pyrolysis product as purified megaspores of *I. killipii* but lacked both benzaldehyde and acetophenone. This

suggests that although *p*-coumaric acid is indeed an important constituent, additional aromatic components, associated with acetophenone and benzaldehyde as pyrolysates, must also be part of the sporopollenin structure (cf. Li et al., 2018).

Another series of components identified, guaiacol (2-methoxyphenol), 4-methyl- and 4-ethylguaiacol, together with the aforementioned 4-vinylguaiacol (Supplement Fig. S4), are typical products found when lignin is present. However, the most distinct pyrolysis products of intact lignin, the three isomers of 4-propenylguaiacol, were not detected (Saiz-Jimenez and De Leeuw, 1984; Ralph and Hatfield, 1991). Hence, guaiacol, 4-methylguaiacol, and 4-ethylguaiacol likely originate from another polyphenol source. The most probable contributors are ferulic acid-rich sporopollenin (*Lycopodium*) or tannin-rich species such as *Betula* and *Eucalyptus* (Galetti and Reeves, 1992). These compounds are present in the other three species in substantially lower amounts (Supplement Fig. S4).

Alkylbenzenes and alkylphenols can have multiple sources such as tannins and proteins (Tsuge and Matsubara, 1985, Bracewell and Robertson, 1984; Galletti and Reeves, 1992). Since all N-bearing components (i.e., proteins) were absent after HF-HCl and acetolysis treatments, the relative accumulation of alkylbenzenes and alkylphenols upon treatment implies a major sporopollenin source of these pyrolysis products.

4.3 The δ^{13}C composition of (un)treated sporomorphs

Overall isotopic composition

The δ^{13}C value of the sporomorphs is essentially a weighted average of the δ^{13}C of all the aforementioned chemical components, broadly divided into polysaccharides/sugars, lipids, proteins and aromatic structures (cf. Hayes, 2001). Except for *Eucalyptus* and *Lolium*, untreated sporomorph species differ significantly from each other in their mean δ^{13}C values (Fig. 3), reflecting the different chemical compositions among the studied species, as well as differences in altitude, humidity, photosynthetic pathways (C_4 [*Zea*] *vs*. C_3 [other species]) and other environmental growth conditions that influence carbon isotope fractionation, from the CO_2 that is taken up to the sporomorph formed (Diefendorf et al., 2010; Farquhar et al., 1982; O'Leary, 1981).

Saponification

The general δ^{13}C increase in saponified sporomorphs compared to untreated samples aligns with the fact that lipids typically have δ^{13}C values 3 – 6‰ lower than bulk biomass (Abelson & Hoering, 1961; Hayes, 2001). This offset reflects the fractionation along the metabolic pathways involved in lipid synthesis which uses acetyl co-enzyme A (acetyl-CoA) as the carbon donor for the lipid skeleton (Hayes, 2001). Acetyl-CoA is produced through pyruvate dehydrogenase, which is known to generate substantial isotopic fractionation (DeNiro & Epstein, 1977; Melzer & Schmidt, 1987). Removal of lipids thus results in the δ^{13}C value of the remaining material to increase. This isotopic effect of saponification contrasts with the findings of Müller et al. (2021), who found a relative δ^{13}C drop of pollen after KOH treatment. Evidently, the use of methanol and DCM in addition to KOH during our saponification treatment resulted in a more effective extraction of lipids, causing the observed δ^{13}C increase. The LA-IRMS measurements of saponified samples show no significant rise in δ^{13}C relative to

untreated pollen, which is likely due to the relatively small sample size ($n = $ ~30, as compared to the EA-IRMS method, which measures >1000 sporomorphs in a single measurement), causing the standard errors of the means to be too large to statistically detect a potential significant offset.

450

HF-HCl

Considering most of the hydrolysable compounds of the sporomorph consist of polysaccharides, which are generally ^{13}C-enriched as compared to total biomass (Hayes, 2001; van Dongen et al., 2002), HF-HCl treatment logically results in lower sporomorph $\delta^{13}C$. Proteins generally have high $\delta^{13}C$ compared that of total biomass (Hayes, 2001; Abelson and Hoering, 1961).

455   However, the $\delta^{13}C$ variation among individual amino acids is large (up to 25‰, Abelson and Hoering, 1961; Macko et al., 1987). This variation arises from the interplay between the sources of the carbon skeletons (e.g., the tricarboxylic acid cycle, pyruvate, or phosphoglycerate) and the isotopic fractionation occurring at metabolic branch points during amino acid biosynthesis (see Hayes [2001] for an in-depth discussion on ^{13}C fractionation during amino acid biosynthesis). Polypeptide $\delta^{13}C$ can therefore theoretically be higher, lower or similar to total biomass $\delta^{13}C$ values (Blair et al., 1985; Abelson and

460   Hoering, 1961; Benner et al., 1987). Due to the relatively small amount of N-bearing compounds present in the sporomorphs, the isotopic effect of HF-HCl is rather dominated by the removal of polysaccharides, i.e., a depletion of the residual sporomorph. The removal of polysaccharides clearly has a substantial effect on $\delta^{13}C$ values (HF-HCl treatment in Fig. 3), even though the pyrolysis based chemical compositions of HF-HCl treated and untreated samples appear similar (Fig. 2). This is likely due to the aforementioned under-detection of polysaccharides with the Py-GC-MS method applied.

465

Acetolysis

Interestingly, for all species, acetolysis results in even more ^{13}C-depleted sporomorphs than HF-HCl (Fig. 3), in line with Müller et al. (2021). This depletion suggests that the residual aromatic components in the sporomorph have a lower $\delta^{13}C$ value than the extractable lipids. Genetic studies (Grienenberger et al., 2011; Zhu et al., 2021) in plants identified specific genes

470   involved in exine formation. These genes encode reductase and synthase enzymes that catalyze the production of tetraketide α-pyrone, a cyclic compound, from medium- to long-chain fatty acids. Tetraketide α-pyrone is believed to serve as an important precursor for sporopollenin suggesting that the precursor of sporopollenin is a fatty acid (Grienenberger et al., 2011; Kim & Douglas, 2013; Zhu et al., 2021). Like fatty acids and other lipids, the biosynthesis of tetraketide α-pyrones relies metabolically on acetyl-CoA, which, as described above, generates substantial ^{13}C fractionation through the pyruvate dehydrogenase reaction

475   involved in its production (DeNiro & Epstein, 1977; Melzer & Schmidt, 1987). Therefore, the relatively low $\delta^{13}C$ values of the aromatic compounds as compared to lipids, can be explained by this additional acetyl-CoA induced fractionation.

4.4 EA-IRMS versus LA-IRMS

For the EA-IRMS measurements, some natural and analytical variability in $\delta^{13}C$ values is evident from the spread in the untreated samples. Particularly for *Zea* and *Lolium*, which have a substantially larger spread than the standard deviation of the

480   GQ standard (0.07‰), it is clear the untreated pollen were not entirely homogeneous before measuring, resulting in some natural variability contributing to the observed variability in the EA-IRMS measurements. However, the even larger spread recorded for acetolyzed pollen (e.g., *Pinus* and *Zea*) is likely due to non-uniform treatment of the material when, for example, the duration of contact between sporomorphs and the acetolysis solution differs for individual sporomorphs, affecting both the composition and amount of removed substances (Hemsley et al., 1993). Except for saponified *Zea* the mean LA- and EA-

485   IRMS $\delta^{13}C$ measurements are not significantly different.

     For saponified *Zea*, the significant difference between the LA- and EA-IRMS means suggests something is measured differently among the two methods. Light microscopy photos show the coloration of the saponified pollen to be more variable than untreated pollen (Supplement Fig. S6), which is possibly represented by the skew to lower $\delta^{13}C$ values witnessed for the distribution of saponified *Zea*. However, the reason behind this EA/LA mismatch remains elusive. An additional PLA

490   correction does not significantly change this result (Supplement Fig. S9).

     Overall, LA-IRMS is the preferred method to study mean $\delta^{13}C$ of sporomorph populations due to more direct targeting of individual or very few specimens, avoiding the isotopic incorporation of non-sporomorph material (e.g., anther fragments) also present in samples. Furthermore, the advantage of LA-IRMS over EA-IRMS is that it enables the analysis of inter-specimen variability and community structure. This is exemplified by the – larger than analytical error – spread of untreated

495   *Zea* and *Lolium* in this study, representing intraspecific differences in carbon isotope ecology, and further highlighted by Frieling et al. (2023), Sluijs et al. (2018) and Van Roij et al. (2017).

4.5 Implications for fossil sporomorphs

The sporopollenin-rich sporomorph left behind after acetolysis can be considered similar to diagenetically altered sporomorphs from the geological record: most labile and hydrolysable components are removed, and only the most durable material remains.

500   However, sporopollenin is also known to be chemically altered during thermal maturation (Watson et al., 2012; Yule et al., 2000). Hydrous pyrolysis (Watson et al., 2012) – simulating thermal maturation – and micro Fourier-transform infrared (FT-IR) analysis (Yule et al., 2000) of gradually heated *Lycopodium* spores reveal a stepwise change in composition of sporopollenin during thermal maturation. Firstly, the ester-bound *n*-carboxylic acids – as represented by the abundant fatty acids found on the exine – are hydrolyzed and polymerized into alkyl groups, increasing the aliphatic proportion of

505   sporopollenin. Secondly, at higher temperature these aliphatic components are thermally cracked, resulting in a relative enrichment of the more stable aromatic components within the residual sporopollenin. Therefore, the stage of maturation determines whether the sporopollenin geopolymer is aliphatic- or aromatic-dominated.

     Considering our results, this implies sporomorph diagenesis may result in stable carbon isotopic fractionation in fossil sporomorphs between that observed in HF-HCl treated (i.e., early stage of maturation, dominated by lipids and aromatics) and

510   acetolyzed (i.e., late mature stage, dominated by aromatics) sporomorphs. According to our results, this means that fossilized sporomorphs, irrespective of the stage of maturation, are always ^{13}C-depleted relative to fresh specimens (Fig. 3).

However, it should be emphasized that the acetolysis procedure affects the material non-uniformly (Hemsley et al., 1993), which increases variation between individual sporomorphs and hence the observed variability in our $\delta^{13}C$ measurements (Fig. 4). Moreover, acetolysis has been shown to alter the sporopollenin structure by removal and addition of C-bearing compounds (Dominguez et al., 1998; Jardine et al., 2017, 2023; Wang et al, 2023), and this is reflected by the substantial decrease in $\delta^{13}C$ associated with acetolysis (Fig. 3), also in comparison to methods that specifically isolate sporopollenin – which acetolysis does not do *per se* (Amundson et al., 1997; Loader and Hemming, 2000). These methods include a cellulase containing enzymic treatment (Li et al., 2019; Lutzke et al., 2020), and acidolysis using sulfuric acid (Loader and Hemming, 2000) and phosphoric acid (Lutzke et al., 2020) – which we advise to use instead of acetolysis, as these do not introduce C-bearing compounds.

However, considering the removal of lipids only minimally affects $\delta^{13}C$ values, as witnessed for saponified compared to untreated sporomorphs (Fig. 3), we propose that the $\delta^{13}C$ depletion associated with the HF-HCl treatment generally corresponds to the carbon isotopic fractionation associated with fossilization of sporomorphs. This implies that the HF-HCl procedure is an appropriate treatment when comparing $\delta^{13}C$ values among modern and fossil sporomorphs.

5 Conclusions

The chemical composition of modern sporomorphs as determined by flash pyrolysis is dominated by lipids (i.e., mostly C_{16} and C_{18} fatty acids), followed by aromatics and polysaccharides, the order of which depends on plant species, with minimal amounts of proteins. After removal of extractable and esterified lipids and hydrolysable polysaccharides and proteins, the sporomorph is dominated by aromatic compounds, which are thought to represent the components of the resistant sporopollenin structure. In addition to present literature, our study shows the composition of this sporopollenin is variable among species. However, *p*-coumaric and ferulic acid are consistent building blocks, whereas the carbonylbenzenes benzaldehyde and acetophenone seem to be unique markers of sporopollenin upon pyrolysis.

Overall, the LA- and EA-IRMS methods agree, meaning the average $\delta^{13}C$ of individually measured sporomorphs is in the line with the bulk value. However, LA-IRMS is the preferred method for $\delta^{13}C$ measurements due to more accurate targeting of the sporomorphs, the possibility to study inter-specimen variability and community structure, and the low amounts of material needed to get an accurate measurement. To take linear mass bias into account when correcting the data, we do advise to use multiple standards across a range of $\delta^{13}C$ values that ideally bracket the range of the data (e.g., PE and PLA).

Both LA- and EA-IRMS illustrate that saponification slightly increases $\delta^{13}C$ values by removal of surface-bound lipids, HF-HCl decreases $\delta^{13}C$ values by removal of polysaccharides and proteins, and acetolysis causes an even more pronounced decrease in $\delta^{13}C$ values, by concentrating the relatively ^{13}C depleted sporopollenin. A combination of HF-HCl treatment and a lipid removal step appears to be the most effective method for investigating the $\delta^{13}C$ value of sporopollenin specifically, as acetolysis seems to chemically alter sporopollenin. Fossil sporomorphs likely have a $\delta^{13}C$ value somewhere between HF-HCl treated and acetolyzed samples of fresh sporomorphs, depending on the stage of maturation, which influences the relative amount of aliphatic lipids as compared to aromatics.

Data availability. All newly generated data will be available via a permanent online repository (Zenodo https://doi.org/10.5281/zenodo.15174422, Bats, 2025) upon publication.

Supplement.

Author contributions. AS and KGJN designed the study. LvR, ASL, JF, KGJN and YFB processed samples and generated data. YFB, KGJN and AS analyzed data. YFB wrote the original draft. AS, KGJN, JF and GJR reviewed and edited the paper. AS and GJR received funding for this study.

Competing interests. The communicating author has declared that none of the authors has any competing interests.

Disclaimer.

Acknowledgements. We thank Arnold van Dijk, Desmond Eefting, Natasja Welters and Giovanni Dammers (Utrecht University) for technical and analytical assistance, and Francien Peterse for valuable discussions.

Financial support. We thank the Ammodo Foundation for funding unfettered research by laureate Appy Sluijs. Appy Sluijs acknowledges funding from European Research Council ERC consolidator grant 771497 (SPANC). This work was supported by EMBRACER (Summit Grant SUMMIT.1.034), financed by the Netherlands Organization for Scientific Research (NWO). This work was carried out under the program of the Netherlands Earth System Science Centre (NESSC); has been financially supported by the Ministry of Education, Culture, and Science (OCW) through Gravitation (grant no. 024.002.001); and has received funding from the European Union's Horizon 2020 research and innovation program under the Marie Skłodowska-Curie Actions (grant no. 847504).

Review statement.

References

Abelson, P. H., & Hoering, T. C. Carbon isotope fractionation in formation of amino acids by photosynthetic organisms. Proceedings of the National Academy of Sciences, 47(5), 623–632. https://doi.org/10.1073/pnas.47.5.623, 1961.

Amundson, R., Evett, R. R., Jahren, A. H., and Bartolome, J.: Stable carbon isotope composition of Poaceae pollen and its potential in paleovegetational reconstructions, Review of Palaeobotany and Palynology, 99, 17-24, https://doi.org/10.1016/S0034-6667(97)00031-6, 1997.

Askin, R.A., Jacobson, S.R., in Encyclopedia of Physical Science and Technology (Third Edition), Meyers, R.A. (ed). ISBN-13: 9780122274107, 2003.

Bats, Y. F. (2025). Pyrolysis and EA- and LA-IRMS measurements of chemically treated pollen, Zenodo [Data set], https://doi.org/10.5281/zenodo.15174422, 2025.

580   Benner, R., Fogel, M. L., Sprague, E. K., and Hodson, R. E.: Depletion of 13C in lignin and its implications for stable carbon isotope studies, Nature, 329, 708-710, 10.1038/329708a0, 1987.

Boom, A., p-Coumaric acid-based sporopollenin of Isoëtes killipii megaspores. In: A geochemical study of lacustrine sediments: towards palaeo-climatic reconstructions of high Andean biomes in Colombia, PhD thesis, University of Amsterdam, pp. 89-101, 2004.

585   Bracewell, J.M., and Robertson, G.W., Quantitative comparison of the nitrogen-containing pyrolysis products and amino acid composition of soil humic acids. Journal of Analytical and Applied Pyrolysis 6, 19-29. https://doi.org/10.1016/0165-2370(84)80002-9, 1984.

Canty, A. and Ripley, B. Boot: Bootstrap R (S-Plus) Functions. R Package Version 1.3-28.1, https://cran.r-project.org/web/packages/boot/boot.pdf, 2022.

590   De Leeuw, J.W., Versteegh, G.J.M., Van Bergen, P.F.: Biomacromolecules of algae and plants and their fossil analogues. Plant Ecol. 182, 20–233, https://doi.org/10.1007/978-1-4020-4443-4_14, 2006.

DeNiro, M. J., & Epstein, S. Mechanism of Carbon Isotope Fractionation Associated with Lipid Synthesis. Science, 197(4300), 261–263. https://doi.org/10.1126/science.327543, 1977.

Descolas-Gros, C., and Schölzel, C.: Stable isotope ratios of carbon and nitrogen in pollen grains in order to characterize
595   plant functional groups and photosynthetic pathway types, New Phytologist, 176, 390-401, https://doi.org/10.1111/j.1469-8137.2007.02176.x, 2007.

Diefendorf, A. F., Mueller, K. E., Wing, Scott. L., Koch, P. L., & Freeman, K. H. Global patterns in leaf13 C discrimination and implications for studies of past and future climate. Proceedings of the National Academy of Sciences, 107(13), 5738–5743, https://doi.org/10.1073/pnas.0910513107, 2010.

600   Domínguez, E., Mercado, J. A., Quesada, M. A., & Heredia, A. Isolation of intact pollen exine using anhydrous hydrogen fluoride. Grana, 37(2), 93-96. https://doi.org/10.1080/00173139809362649, 1998.

Erdtman, G.: The acetolysis method. A revised description. - Svensk Bot. Tidskr. 54, 561 - 564, 1960

Fan, T.-F., Potroz, M. G., Tan, E.-L., Ibrahim, M. S., Miyako, E., and Cho, N.-J.: Species-Specific Biodegradation of Sporopollenin-Based Microcapsules, Scientific Reports, 9, 9626, 10.1038/s41598-019-46131-w, 2019.

605 Farquhar, G., O'Leary, M., & Berry, J. On the Relationship Between Carbon Isotope Discrimination and the Intercellular Carbon Dioxide Concentration in Leaves. Functional Plant Biology, 9(2), 121. https://doi.org/10.1071/PP9820121, 1982.

Fensome, R. A., Taylor, F. J. R., Norris, G., Sarjeant, W. A. S., Wharton, D. I., and Williams, G. L.: A Classification of Fossil and Living Dinoflagellates, Micropaleontology, Special Publication, 351p. pp., 1993.

Frieling, J., Van Roij, L., Kleij, I., Reichart, G.-J., & Sluijs, A. Single-species dinoflagellate cyst carbon isotope fractionation 610 in core-top sediments: Environmental controls, CO_2 dependency and proxy potential. Biogeosciences, 20(22), 4651–4668. https://doi.org/10.5194/bg-20-4651-2023, 2023.

Galletti, G.C., Reeves, J.B., Pyrolysis/gas chromatography/ion trap detection of polyphenols (vegetable tannins): preliminary results. Organic Mass Spectrometry 27, 226-230. https://doi.org/10.1002/oms.1210270313 1992.

Grienenberger, E., Kim, S. S., Lallemand, B., Geoffroy, P., Heintz, D., Souza, C. de A., Heitz, T., Douglas, C. J., & Legrand, 615 M. Analysis of TETRAKETIDE α-PYRONE REDUCTASE Function in Arabidopsis thaliana Reveals a Previously Unknown, but Conserved, Biochemical Pathway in Sporopollenin Monomer Biosynthesis. The Plant Cell, 22(12), 4067– 4083. https://doi.org/10.1105/tpc.110.080036, 2011.

H. Wickham. ggplot2: Elegant Graphics for Data Analysis. Springer-Verlag New York, 2016.

Hayes, J. M. Fractionation of the Isotopes of Carbon and Hydrogen in Biosynthetic Processes. Reviews in Mineralogy & 620 Geochemistry, 43, 225–273, https://doi.org/10.2138/gsrmg.43.1.225, 2001.

Hemsley, A. R., Barrie, P. J., Chaloner, W. G., & Scott, A. C. The composition of sporopollenin and its use in living and fossil plant systematics. Grana, 32(S1), 2-11. https://doi.org/10.1080/00173139309427446, 1993.

Hesse, M., and Waha, M.: A new look at the acetolysis method. P1. Syst. Evol. 163, 147-152, 1989.

Hoins, M., Van de Waal, D. B., Eberlein, T., Reichart, G.-J., Rost, B., and Sluijs, A.: Stable carbon isotope fractionation of 625 organic cyst-forming dinoflagellates: Evaluating the potential for a CO_2 proxy, Geochim Cosmochim Ac, 160, 267-276, http://dx.doi.org/10.1016/j.gca.2015.04.001, 2015.

Jahren, A. H.: The carbon stable isotope composition of pollen, Review of Palaeobotany and Palynology, 132, 291-313, https://doi.org/10.1016/j.revpalbo.2004.08.001, 2004.

Jardine, P.E., Abernethy, F.A.J., Lomax, B.H., Gosling, W.D., and Fraser, W.T. Shedding light on sporopollenin chemistry, with reference to UV reconstructions. Rev. Palaeobot. Palynol. 238, 1–6. https://doi.org/10.1016/j.revpalbo.2016.11.014, 2017.

Jardine, P.E., Hoorn, C., Beer, M.A.M., Barbolini, N., Woutersen, A., Bogota-Angel, G., Gosling, W.D., Fraser, W.T., Lomax, B.H., Huang, H., Sciumbata, M., He, H. and Dupont-Nivet. Sporopollenin chemistry and its durability in the geological record: an integration of extant and fossil chemical data across the seed plants. Palaeontology 64, 285-305. https://doi: 10.1111/pala.12523, 2021.

Jardine, P. E., Kent, M. S., Fraser, W. T., Knorr, K. H., & Lomax, B. H. Uncovering a phylogenetic signal in plant biopolymer chemistry: a comparison of sporopollenin isolation approaches for use in palynological research. Palaeontology, 66(6), e12683. https://doi.org/10.1111/pala.12683, 2023.

Kaufman, A. J., & Xiao, S. High CO2 levels in the Proterozoic atmosphere estimated from analyses of individual microfossils. Nature, 425(6955), 279–282. https://doi.org/10.1038/nature01902, 2003.

Kim, S. S., & Douglas, C. J. Sporopollenin monomer biosynthesis in arabidopsis. Journal of Plant Biology, 56(1), 1–6. https://doi.org/10.1007/s12374-012-0385-3, 2013.

Li, F.-S., Phyo, P., Jacobowitz, J., Hong, M., and Weng, J.-K. The molecular structure of plant sporopollenin. Nat. Plants 5, 41–46. https://doi.org/10.1038/s41477-018-0330-7, 2019.

Loader, N. J., and Hemming, D. L.: Preparation of pollen for stable carbon isotope analyses, Chemical Geology, 165, 339-344, https://doi.org/10.1016/S0009-2541(99)00176-X, 2000.

Loader, N. J., and Hemming, D. L.: The stable isotope analysis of pollen as an indicator of terrestrial palaeoenvironmental change: a review of progress and recent developments, Quaternary Science Reviews, 23, 893-900, https://doi.org/10.1016/j.quascirev.2003.06.015, 2004.

Lutzke, A., Morey, K. J., Medford, J. I. and Kipper, M. J. Detailed characterization of Pinus ponderosa sporopollenin by infrared spectroscopy. Phytochemistry, 170, 112195. https://doi.org/10.1016/j.phytochem.2019.112195, 2020.

Melzer, E., & Schmidt, H. L. Carbon isotope effects on the pyruvate dehydrogenase reaction and their importance for relative carbon-13 depletion in lipids. Journal of Biological Chemistry, 262(17), 8159–8164. https://doi.org/10.1016/S0021-9258(18)47543-6, 1987.

Moldoveanu, S.C., Analytical Pyrolysis of Natural Organic Polymers, 1st Ed. Elsevier, 623 pp., ISBN: 0-444-82203-8, 1989.

Müller, C., Hennig, J., Riedel, F., and Helle, G.: Quantifying the impact of chemicals on stable carbon and oxygen isotope values of raw pollen, Journal of Quaternary Science, 36, 441-449, https://doi.org/10.1002/jqs.3300, 2021.

Murphey, B. F., and Nier, A. O.: Variations in the Relative Abundance of the Carbon Isotopes, Physical Review, 59, 771-772, 10.1103/PhysRev.59.771.2, 1941.

660   Nelson, D. M., Hu, F. S., and Michener, R. H.: Stable-carbon isotope composition of Poaceae pollen: an assessment for reconstructing C3 and C4 grass abundance, The Holocene, 16, 819-825, 10.1191/0959683606hol974rp, 2006.

Nelson, D. M., Hu, F. S., Mikucki, J. A., Tian, J., and Pearson, A.: Carbon-isotopic analysis of individual pollen grains from C3 and C4 grasses using a spooling-wire microcombustion interface, Geochim Cosmochim Ac, 71, 4005-4014, 2007.

Nierop, K.G.J., Speelman, E.E., De Leeuw, J.W., and Reichart, G.J.: The omnipresent water fern Azolla caroliniana does not
665   contain lignin. Organic Geochemistry 42, 846-850. https://doi.org/10.1016/j.orggeochem.2011.05.001, 2011.

Nierop, K.G.J., Versteegh, G.J.M., Filley, T.R., and De Leeuw, J.W.: Quantitative analysis of diverse sporomorph-derived sporopollenins. Phytochemistry 162, 207-215, doi:10.1016/j.phytochem.2019.03.023, 2019.

O'Leary, H. CARBON ISOTOPE FRACTIONATION IN PLANTS. Phytochemistry, 20(4), 553–567, https://doi.org/10.1016/0031-9422(81)85134-5, 1981.

670   Pacini, E., & Hesse, M. Pollenkitt – its composition, forms and functions. Flora - Morphology, Distribution, Functional Ecology of Plants, 200(5), 399–415. https://doi.org/10.1016/j.flora.2005.02.006, 2005.

Polissar, P. J., Fulton, J. M., Junium, C. K., Turich, C. C., and Freeman, K. H.: Measurement of 13C and 15N Isotopic Composition on Nanomolar Quantities of C and N, Analytical Chemistry, 81, 755-763, 10.1021/ac801370c, 2009.

Quilichini, T.D., Grienenberger, E., Douglas, C.J.: The biosynthesis, composition and assembly of the outer pollen wall: A
675   tough case to crack. Phytochem. 113, 170-182, http://dx.doi.org/10.1016/j.phytochem.2014.05.002, 2015.

R Core Team. _R: A Language and Environment for Statistical Computing_. R Foundation for Statistical Computing, Vienna, Austria, https://www.R-project.org/, 2023.

Schilder, J., Van Roij, L., Reichart, G.-J., Sluijs, A., and Heiri, O.: Variability in δ13C values between individual Daphnia ephippia: Implications for palaeo-studies, Quaternary Science Reviews, 189, 127-133,
680   https://doi.org/10.1016/j.quascirev.2018.04.007, 2018.

Sessions, A. L., Sylva, S. P., and Hayes, J. M.: Moving-Wire Device for Carbon Isotopic Analyses of Nanogram Quantities of Nonvolatile Organic Carbon, Analytical Chemistry, 77, 6519-6527, 10.1021/ac051251z, 2005.

Shim, S.-H., Mahong, B., Lee, S.-K., Kongdin, M., Lee, C., Kim, Y.-J., Qu, G., Zhang, D., Ketudat Cairns, J. R., & Jeon, J.-S. Rice β-glucosidase Os12BGlu38 is required for synthesis of intine cell wall and pollen fertility. Journal of Experimental
685   Botany, 73(3), 784–800. https://doi.org/10.1093/jxb/erab439, 2022.

Sluijs, A., van Roij, L., Frieling, J., Laks, J., and Reichart, G.-J.: Single-species dinoflagellate cyst carbon isotope ecology across the Paleocene-Eocene Thermal Maximum, Geology, 46, 79-82, 10.1130/G39598.1, 2018.

Tsuge, S., Matsubara, H., High-resolution pyrolysis-gas chromatography of proteins and related materials. Journal of Analytical and Applied Pyrolysis 8, 49-64. https://doi.org/10.1016/0165-2370(85)80014-0. 1985.

Van Bergen, P.F., Collinson, M.E., and De Leeuw, J.W., Chemical composition and ultrastructure of fossil and extant salvinialean microspore massulae and megaspores. Grana, 32:S1, 18-30, DOI: 10.1080/00173139309427448, 1993.

Van Dongen, B., Schouten, S., & Sinninghe Damsté, J. Carbon isotope variability in monosaccharides and lipids of aquatic algae and terrestrial plants. Marine Ecology Progress Series, 232, 83–92. https://doi.org/10.3354/meps232083, 2002.

Van Hardenbroek, M., Chakraborty, A., Davies, K. L., Harding, P., Heiri, O., Henderson, A. C. G., Holmes, J. A., Lasher, G. E., Leng, M. J., Panizzo, V. N., Roberts, L., Schilder, J., Trueman, C. N., and Wooller, M. J.: The stable isotope composition of organic and inorganic fossils in lake sediment records: Current understanding, challenges, and future directions, Quaternary Science Reviews, 196, 154-176, https://doi.org/10.1016/j.quascirev.2018.08.003, 2018.

Van Hardenbroek, M., Heiri, O., Grey, J., Bodelier, P. L. E., Verbruggen, F., and Lotter, A. F.: Fossil chironomid $\delta13C$ as a proxy for past methanogenic contribution to benthic food webs in lakes?, Journal of Paleolimnology, 43, 235-245, 10.1007/s10933-009-9328-5, 2010.

Van Roij, L., Sluijs, A., Laks, J. J., and Reichart, G.-J.: Stable carbon isotope analyses of ng quantities of particulate organic carbon (pollen) with laser ablation nano combustion gas chromatography isotope ratio mass spectrometry, Rapid Communications in Mass Spectrometry, 31, 47-58, 10.1002/rcm.7769, 2017.

Versteegh, G. J. M., Blokker, P., Marshall, C., and Pross, J.: Macromolecular composition of the dinoflagellate cyst Thalassiphora pelagica (Oligocene, SW Germany), Org Geochem, 38, 1643-1656, 2007.

Wang, T., Bell, B. A., Fletcher, W. J., Ryan, P. A., & Wogelius, R. A. Influence of common palynological extraction treatments on ultraviolet absorbing compounds (UACs) in sub-fossil pollen and spores observed in FTIR spectra. Frontiers in Ecology and Evolution, 11: 1096099. https://doi.org/10.3389/fevo.2023.1096099, 2023.

Watson, J. S., Fraser, W. T., & Sephton, M. A. Formation of a polyalkyl macromolecule from the hydrolysable component within sporopollenin during heating/pyrolysis experiments with Lycopodium spores. Journal of Analytical and Applied Pyrolysis, 95, 138–144. https://doi.org/10.1016/j.jaap.2012.01.019, 2012.

Wickham H, François R, Henry L, Müller K, Vaughan D. _dplyr: A Grammar of Data Manipulation_. R package version 1.1.4, https://CRAN.R-project.org/package=dplyr, 2023.

Wickham H, Vaughan D, Girlich M. _tidyr: Tidy Messy Data_. R package version 1.3.0, https://CRAN.R-project.org/package=tidyr, 2023.

Wilke C. _ggridges: Ridgeline Plots in 'ggplot2'_. R package version 0.5.6, 2024.

Wooller, M. J.: The stable isotope composition of organic and inorganic fossils in lake sediment records: Current understanding, challenges, and future directions, Quaternary Science Reviews, 196, 154-176, https://doi.org/10.1016/j.quascirev.2018.08.003, 2018.

Yule, B. L., Roberts, S., & Marshall, J. E. A. The thermal evolution of sporopollenin. Organic Geochemistry, 31(9), 859–870. https://doi.org/10.1016/S0146-6380(00)00058-9, 2000.

Zhu, L., Zhang, T., & Teeri, T. H. Tetraketide α-pyrone reductases in sporopollenin synthesis pathway in Gerbera hybrida: Diversification of the minor function. Horticulture Research, 8, 207. https://doi.org/10.1038/s41438-021-00642-8, 2021.